

# SYNCHRONIZATION IN CHAINS OF VAN DER POL OSCILLATORS

**Andreas Henrici**

ZHAW School of Engineering  
Technikumstrasse 9  
CH-8401 Winterthur, Switzerland  
andreas.henrici@zhaw.ch

**Martin Neukom**

ZHdK ICST  
Toni-Areal, Pfingstweidstrasse 96  
CH-8031 Zürich, Switzerland  
martin.neukom@zhdk.ch

## ABSTRACT

In this paper we describe some phenomena arising in the dynamics of a chain of coupled van der Pol oscillators, mainly the synchronisation of the frequencies of these oscillators, and provide some applications of these phenomena in sound synthesis.

## 1. INTRODUCTION

If several distinct natural or artificial systems interact with each other, there is a tendency that these systems adjust to each other in some sense, i.e. that they synchronize their behavior. Put more precisely, by synchronization we mean (following [1]) the *adjustment of the rhythms of oscillating objects due to their mutual interaction*. Synchronization can occur in model systems such as a chain of coupled van der Pol oscillators but also in more complex physical, biological or social systems such as the coordination of clapping of an audience [2]. Historically, synchronization was first described by Huygens (1629-1695) on pendulum clocks [3]. In modern times, major advances were made by van der Pol [4] and Appleton [5]. Physically, we basically distinguish between synchronization by external excitation, mutual synchronization of two interacting systems and synchronization phenomena in chains or topologically more complex networks of oscillating objects. Whereas in [6] we discussed the case of two interacting systems, in this paper, we will focus on the case of a (one-dimensional) chain of oscillators with diffusive nearest-neighbor coupling. For a modern overview of the topic of synchronization, see e.g. [7, 8]; an intuitively well accessible example is the synchronization of metronomes [9, 10].

The synchronizability of such a chain of oscillators depends on several parameters of the system, mainly the detuning between the individual frequencies and the strength of the coupling between the oscillators. It can be observed that before completely synchronizing, the chain forms clusters of neighboring masses with similar frequencies. For growing interaction strength, the size of these clusters increases, whereas their number decreases, before at a certain threshold, the whole chain forms a single cluster, which

corresponds to the state of complete synchronization.

In addition, we consider chains of oscillators where the coupling does not happen instantaneously, but with a delay. Depending on the value of the delay, significant changes in the dynamics of the system can be observed.

Self-sustained oscillators can be used in sound synthesis to produce interesting sounds and sound evolutions in different time scales. A single van der Pol oscillator, depending on only one parameter ( $\mu$ , see (1)), produces a more or less rich spectrum, two coupled oscillators can synchronize after a while or produce beats depending on their frequency mismatch and strength of coupling [11, 12]. In chains or networks of coupled oscillators in addition different regions can synchronize (the clusters mentioned above), which takes even more time. If the coupling is not immediate but after a delay it can take a long time for the whole system to come to a steady or periodic changing state. In addition all these effects can not only be used to produce sound but also to generate mutually dependent parameters of any sound synthesis technique. In a series of studies (Studien 21.1-21.9) one of the authors (Neukom) investigated these effects.

This paper gives an introduction to the synchronization of such oscillator chains [1, 13], using the van der Pol system as primary example. However, similar effects can be observed for other systems.

## 2. CHAINS OF COUPLED VAN DER POL OSCILLATORS

### 2.1 Van der Pol oscillators

Self-sustained oscillators are a model of natural or technical oscillating objects which are active systems, i.e. which contain an inner energy source. The form of oscillation does not depend on external inputs; mathematically, this corresponds to the system being described by an autonomous (i.e. not explicitly time-dependent) dynamical system. Under perturbations, such an oscillator typically returns to the original amplitude, but a phase shift can remain even under weak external forces. Typical examples of self-sustained oscillators are the van der Pol oscillator

$$\begin{aligned}\dot{x} &= y \\ \dot{y} &= -\omega_0^2 x + \mu(1 + \gamma - x^2)y\end{aligned}\quad (1)$$

and the Rössler and Lorenz oscillators. Note that in the van der Pol oscillator (1), the parameters  $\mu$  and  $\gamma$  measure the strength of the nonlinearity; in particular, for  $\mu = 0$

we obtain the standard harmonic oscillator. In the case of a single oscillator we usually set  $\gamma = 0$ , whereas in the case of several oscillators we can use distinct values of  $\gamma$  to describe the amplitude mismatch of the various oscillators. Assuming  $\gamma = 0$ , in the nonlinear case  $\mu \neq 0$ , the term  $\mu(1 - x^2)y$  means that for  $|x| > 1$  and  $|x| < 1$  there is negative or positive damping, respectively.

We will discuss an implementation of the van der Pol model (1) in section 4.

## 2.2 Oscillator Chains

If one considers an entire chain of oscillators, the model equations are for any  $1 \leq j \leq n$

$$\ddot{x}_j + \omega_j^2 x_j = 2\mu(p - x_j^2)\dot{x}_j + 2\mu d(\dot{x}_{j-1} - 2\dot{x}_j + \dot{x}_{j+1}) \quad (2)$$

together with the (free end) boundary conditions

$$x_0(t) \equiv x_1(t), \quad x_{n+1}(t) \equiv x_n(t).$$

Sometimes we also use periodic boundary conditions, i.e.

$$x_0(t) \equiv x_n(t), \quad x_1(t) \equiv x_{n+1}(t).$$

Note that in the oscillator chain (2), the parameters  $d$  measures the strength of the coupling between neighboring oscillators; in particular, for  $d = 0$  we obtain the single oscillator (1), with  $p = 1 + \gamma$ . As we will see in the following section (see e.g. Figure 3), with growing values of  $d$  the oscillators of the chain more likely synchronize.

We assumed different models for the distribution of the frequencies  $\omega_j$  of the  $n$  oscillators, in particular the following ones:

- Linear distribution:

$$\omega_k = \omega_1 + (k - 1)\Delta, \quad (3)$$

depending on the detuning parameter  $\Delta$

- Exponential distribution:

$$\omega_k = \omega_1 + (1 + \Delta)^k, \quad (4)$$

also depending on the detuning parameter  $\Delta$

- Random distribution:

$$\omega_k \sim U(\omega_{\min}, \omega_{\max}), \quad (5)$$

i.e. the  $\omega_k$ 's are independent random variables all being distributed uniformly in a certain interval.

We first discuss the linear case (3). In this case, an analytic discussion can be carried out in the case of weak coupling, i.e.  $d \ll 1$  in (2). One can show (see e.g. [13]) that in this case, the second order system (2) can be rewritten as the first order system

$$\dot{z}_j = i\Delta_j z_j + (p - |z_j|^2)z_j + d(z_{j+1} - 2z_j + z_{j-1}) \quad (6)$$

for complex variables  $z_j$ , which turns out to be a spatial discretization of the Ginzburg-Landau equation. By writing  $z_j = \rho_j e^{i\theta_j}$ , the complex system (6) can then be rewritten as a real system for the amplitudes  $\rho_j$  and phases  $\theta_j$ .

Global synchronization of the original dynamical system (2) then means that this new system for the variables  $\rho_j, \theta_j$  has a stable steady state. One shows that this occurs if the condition

$$\left| \frac{\Delta n^2}{8d} \right| < 1 \quad (7)$$

is satisfied, or put differently, that the coupling parameter  $d$  has to be above the threshold  $\frac{\Delta n^2}{8}$  for the system (2) to be completely synchronized.

## 2.3 Numerical Simulations

In Figure 1, where the  $n$  trajectories are plotted on a  $t - x_j$ -diagram, one observes the complete synchronization of a chain of  $N = 20$  oscillators with linearly distributed frequencies, i.e. according to (3), with  $\Delta = 0.002$ , and with the coupling  $d = 0.5$ . The synchronization condition (7) is clearly satisfied. The initial conditions were chosen randomly in the interval  $[-1, 1]$ . All figures in this section were produced with the pre-implemented methods `ode45`, `ode23s`-and `dde23`-methods of `Matlab`, and in all simulations, we used the values  $\omega_1 = 1$ ,  $p = 0.5$ , and  $\mu = 1$  in (2) and (3).

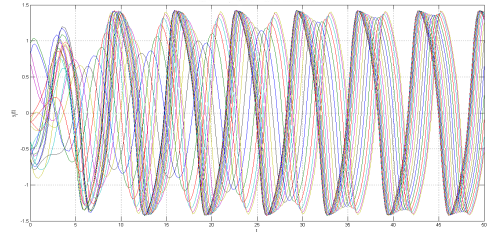


**Figure 1.** Complete synchronization of the van der Pol chain (2) for  $n = 20$ ,  $\Delta = 0.002$ , and  $d = 0.5$

In Figure 2, where the  $n$  trajectories are plotted as colors in a  $j - t$ -diagram, we consider the case of a chain of  $n = 100$  oscillators with linear frequency distribution (3) for the detuning  $\Delta = 0.002$  and the coupling  $d = 2.5$ . The condition (7) is clearly not satisfied, and one can observe the increasing oscillation frequencies for growing  $j$ . One also sees the existence of synchronization clusters, i.e. regions of indices  $j$  where the respective oscillators have the same frequency.

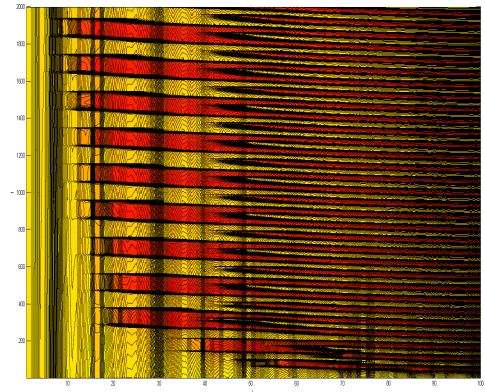


**Figure 2.** Space-time plot of the chain (2) for  $\Delta = 0.002$  and  $d = 2.5$

The transition from the cluster to the synchronization regime can be well seen in the following figure, where for different values of the coupling  $d$  the oscillator frequencies are plotted vs. the index  $j$ :

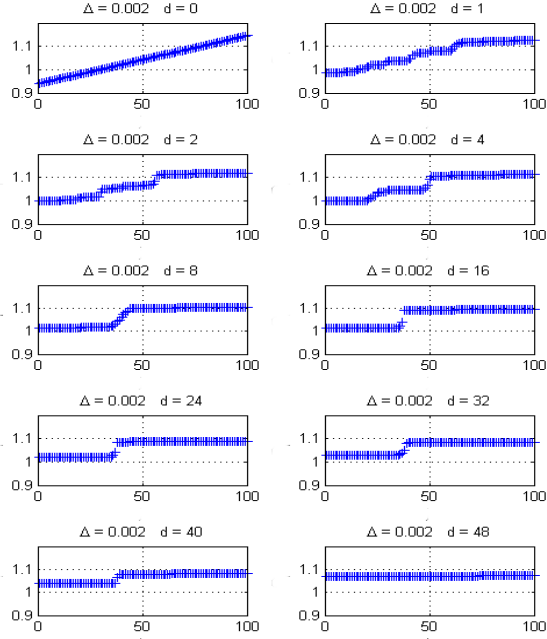


**Figure 3.** Transition from the cluster formation to the synchronization regime for the chain (2): Space-frequency- (i.e.  $j$ - $\omega_j$ -) plots for  $\Delta = 0.002$  and various values of  $d$

Yet another way to describe the process of synchronization for growing coupling strength is by the *synchronization tree* which plots the coupling strength vs. the frequencies:

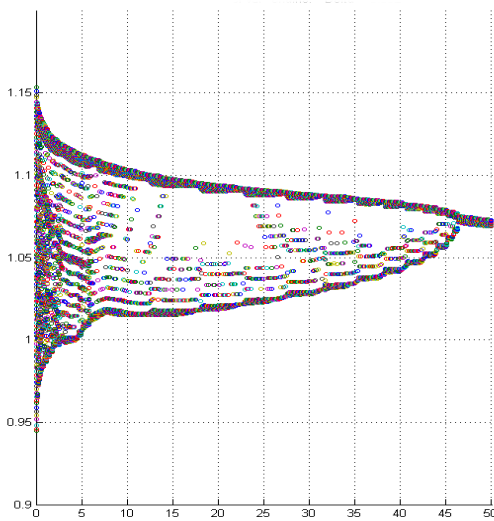


**Figure 4.** Synchronization tree for the chain (2): Coupling-frequencies- (i.e.  $d$ - $\omega_j$ -) plots,  $1 \leq j \leq n$ , with  $\Delta = 0.002$

## 2.4 Influence of delays

If a delay  $\tau$  is introduced into the system (2), we obtain the system of DDE's (delay differential equations)

$$\ddot{x}_j(t) + \omega_j^2 x_j(t) = 2\mu(p - x_j^2(t))\dot{x}_j(t) + 2\mu d(\dot{x}_{j-1}(t - \tau_B) - 2\dot{x}_j(t - \tau_0) + \dot{x}_{j+1}(t - \tau_A)), \quad (8)$$

where  $\tau_0$ ,  $\tau_A$ , and  $\tau_B$  denote the delays from oscillators  $j \rightarrow j$ ,  $j+1 \rightarrow j$  (backward), and  $j-1 \rightarrow j$  (forward). Note that we only consider the simplest situation of the delays being constant. We chose  $\tau_0 = \tau_A = \tau_B =: \tau$  for our numerical experiments and  $\tau_0 = 0$  (no self-delay) and  $\tau_A = \tau_B =: \tau$  for our experiments in Max (see section 3). For a study of a single van der Pol oscillator with delayed self-feedback see [14], and a pair of such oscillators has been investigated in the case without detuning [15]. The assumption of a delayed signal transmission or feedback process is a very natural assumption in certain physical and biological systems, since these transmission and feedback processes in general do not occur instantaneously. For an overview over the dynamics of time-delay systems such as (8), see e.g. [16, 17].

Our experiments show that already small values of  $\tau$  can completely alter pictures such as Figure 2, see Figures 5, 6, and 7 for the cases  $\tau = 0.08$ ,  $\tau = 0.09$  and  $\tau = 0.1$ , respectively.

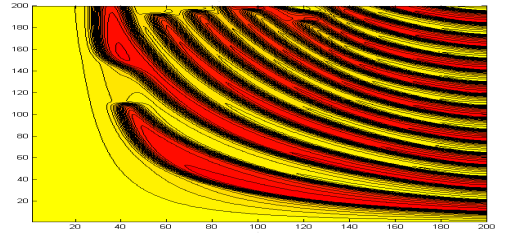


**Figure 5.** Space-time (i.e.  $j$ - $t$ -) plot of the delayed chain (8) for  $n = 200$ ,  $\Delta = 0.002$ ,  $d = 2.5$ ,  $\tau = 0.08$

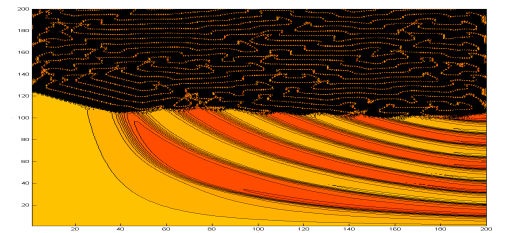


**Figure 6.** Space-time (i.e.  $j$ - $t$ -) plot of the delayed chain (8) for  $n = 200$ ,  $\Delta = 0.002$ ,  $d = 2.5$ ,  $\tau = 0.09$

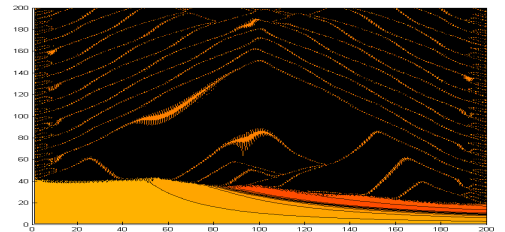


**Figure 7.** Space-time (i.e.  $j$ - $t$ -) plot of the delayed chain (8) for  $n = 200$ ,  $\Delta = 0.002$ ,  $d = 2.5$ ,  $\tau = 0.1$

Whereas in Figure 5 we see a behavior which qualitatively resembles the behavior in the non-delayed case shown in Figure 2, we see in Figures 6 and 7 that after a certain time the delays lead to a distinctly different dynamics of the oscillator chain. Even more than in the non-delayed case, many of these phenomena still defy an analytical explanation.

### 3. APPLICATION IN MAX

#### 3.1 Implementation

In order to experiment in real time we implemented a chain of  $n = 50$  van der Pol oscillators in Max with a visual representation of the oscillator values depending on time and the number of the oscillators and a representation of the frequencies depending on time. Figure 8 shows the main features of the Max patch `smc16_vdp.maxpat` with the external `smc16_vdp_chain` and two plots. The inputs for the external are the frequency in Hz,  $\omega/\text{sr}$ , the nonlinearity  $\mu$ , the delay in samples, the coupling strength  $d$ , the amount of deviation of omega from one oscillator to the next (above called detuning,  $d_\text{omega}$ ) and the random range of the omegas (`rand_omega`). The time step is the sample period. The plots show the oscillation values over time as gray level (left) and the frequencies over time (right).

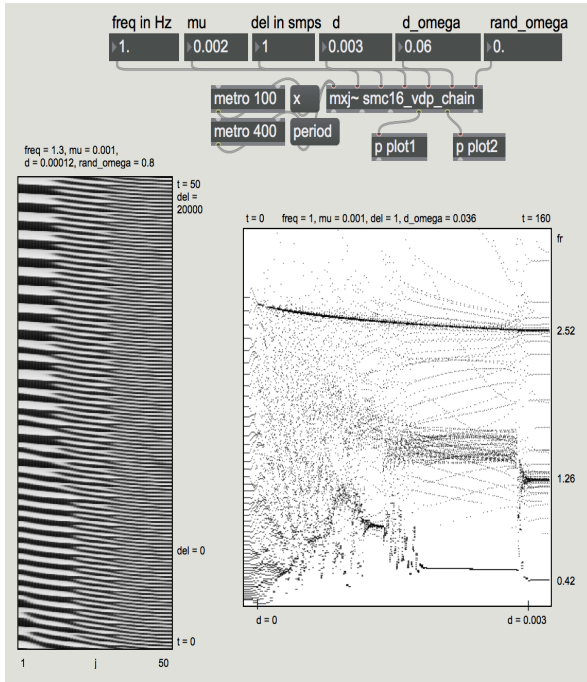


**Figure 8.** Simplified version of the Max patch `smc16_vdp.maxpat`

While for the production of the figures in section 2 we used pre-implemented methods, we will now show explicitly how to obtain discrete systems from the differential equations: first by the Euler method used in Neukom's studies 21.1-21.9 and then the classical Runge-Kutta method implemented in the Max-patch `smc16_vdp.maxpat` which

we used to produce the following figures. The following Java code samples are taken from the `perform` routine of the above mentioned `mxj~` external `smc16_vdp_chain`. The external and the Max patch can be downloaded from [18].

The implementation of Euler's Method for a single van der Pol oscillator is straightforward, the code is short and fast and with the sample period as time step quite precise [11]. First the acceleration  $a$  is calculated according to the differential equation above (1), using the nonlinearity  $\mu$ . Then the velocity  $v$  is incremented by the acceleration times  $dt$  and displacement  $x$  by velocity times  $dt$  ( $dt = 1$ ).

---

```
a = (- c*x + mu*(1 - x*x)*v);
      // with c = (frequency*2*Pi/sr)^2
v += a;
x += v;
```

---

The classical Runge-Kutta method (often referred to as RK4) is a fourth-order method. The values  $x$  and  $v$  of the next sample are approximated in four steps. The following code sample from the `mxj~` external `smc_vdp` shows the calculation of the new values  $x$  and  $v$  using the function `f_` which calculates the acceleration.

---

```
double f_(double x, double v){ return - c*x + mu*(1 - x*x)*v;}

k1 = f_(x, v);
l1 = v;
k2 = f_(x+l1/2, v+k1/2);
l2 = v+k1/2;
k3 = f_(x+l2/2, v+k2/2);
l3 = v+k2/2;
k4 = f_(x+l3, v+k3);
l4 = v+k3;
a = (k1 + 2*k2 + 2*k3 + k4)/6;
v += a;
x += (l1 + 2*l2 + 2*l3 + l4)/6;
```

---

The next code sample shows how a coupling with delay in a chain of  $n$  oscillators is implemented. Acceleration  $a$ , velocity  $v$ , displacement  $x$  and nonlinearity  $\mu$  are stored in arrays of length  $n$ . In this implementation the coupling strength is the same for all connections. The oscillators are coupled by the difference of their own and the delayed velocity of their neighbors. The delay of the velocities is realized with  $n$  circular buffers by the two-dimensional array `delv[n][dmax]` with length  $n$  times the maximal length `dmax` of used delay. The positions where the velocities are written into and read out of the buffers are called `pin` and `pout`, respectively. The additional parts of the acceleration term due to the coupling conditions of the first and last oscillators of the chain are

---

```
d*(delv[1][pout] - v[0]);
d*(delv[n-2][pout] - v[n-1]);
```

---

and for the other oscillators

---

```
d*(delv[k+1][pout] + delv[k-1][pout] - 2*v[k]); // k = 1
to n - 2
```

---

The inputs for the external `smc16_vdp_chain` are the



frequency in Hz, the nonlinearity  $\mu$ , the delay in samples, the coupling  $d$ , the amount of deviation of omega from one oscillator to the next (the detuning  $d\_omega$ , cf. (3)) and the random range of the omegas ( $rand\_omega$ , cf. (5)). From the input frequency we calculate  $omega\_0$  of a corresponding linear oscillator ( $\mu = 0$ ). ( $omega\_0 = (frequency * 2 * \pi / sr)^2$ ). From  $omega\_0$  we get the individual omegas of the  $n$  oscillators either by exponentially or randomly distributing them depending on the input variables  $d\_omega$  and  $rand\_omega$ .

---

```
omega[k] = omega_0*(1 + d_omega*k); // k = 0 to n - 1

omega[k] =
    omega_0*(1+rand_omega*((float)(Math.random()-0.5f)));
    // k = 0 to n-1
```

---

We calculate the position of the index *pout* for reading out the delayed velocities from the position of the index *pin* for writing the current velocities and the input delay *del*:

---

```
pout = pin - del;
```

---

For the following experiments the  $n$  factors  $\mu$  (nonlinearity) and  $d$  (coupling) are identical.

In the visual representation of the oscillator values the  $x$ -axes represents the chain with the 50 oscillators and the  $y$ -axes the time in seconds. Every 100 ms a message triggers the output of the current oscillator values. The values are interpreted as gray level between -1 and 1.

In the visual representation of the evolution of the frequencies the  $x$ -axes represents the time and the  $y$ -axes the frequencies. Every 400 ms a message triggers the output of the current length of the periods of the oscillations.

### 3.2 Experiments

In a series of experiments we investigated chains with random and exponential distribution of the frequencies of the oscillators. We varied the delay and the coupling. Figure 9 shows the evolution of a chain with randomly distributed frequencies ( $rand\_omega = 0.8$ ). During the first 10 seconds there is no coupling, then the coupling grows linearly from 0 to 0.0002. With growing coupling more and more clusters appear where some oscillators synchronize their frequencies and by the time some clusters merge and the frequencies decrease. Figure 10 shows the same chain with the constant coupling 0.0001 and a growing delay. At the beginning of the simulation all oscillators were inactive. The first oscillator was excited by a small impulse. The excitation then propagates along the chain with growing delay. After a few seconds the clusters of synchronized frequencies appear. The phase differences between synchronized oscillators grow with the delay and the stripes in the figure become steeper. When the delay becomes longer than half of a period the delayed velocities of the neighbors of an oscillator have opposite sign to the velocity of this oscillator. As a result neighbors become out of phase and the difference of the velocities and hence the acceleration increase. In Figure 10 this happens at a delay of about 20000

samples where checked pattern begin to dominate; compare this uppermost pair of Figure 10 to the upper parts of Figures 6 and 7.

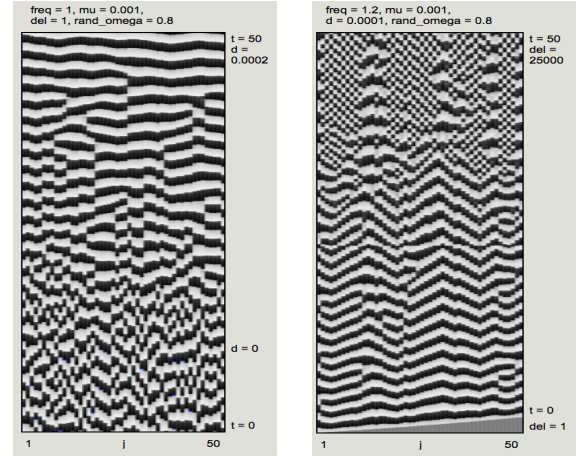


**Figure 9.** Randomly distributed frequencies

**Figure 10.** Constant coupling, growing delay

Figure 11 shows the evolution of a chain with exponentially distributed frequencies ( $d\_omega = 0.06$ , cf. (4)). During the first 8 seconds there is no coupling, then the coupling grows linearly from 0 to 0.004. With growing coupling more and more oscillators synchronize and clusters merge. The low frequencies increase (the stripes on the left side of the figure become smaller) and the high frequencies decrease. The frequencies of the regions become stable and harmonic  $0.42 : 1.26 : 2.52 = 1 : 3 : 6$  (see Figure 11). Figure 12 shows the same chain with the constant coupling 0.002 and a growing delay. After a few seconds the same clusters of synchronized frequencies appear as in the upper part of figure 11. The phase differences between synchronized oscillators grow with the delay and the stripes in the figure become steeper. All the frequencies decrease clearly.

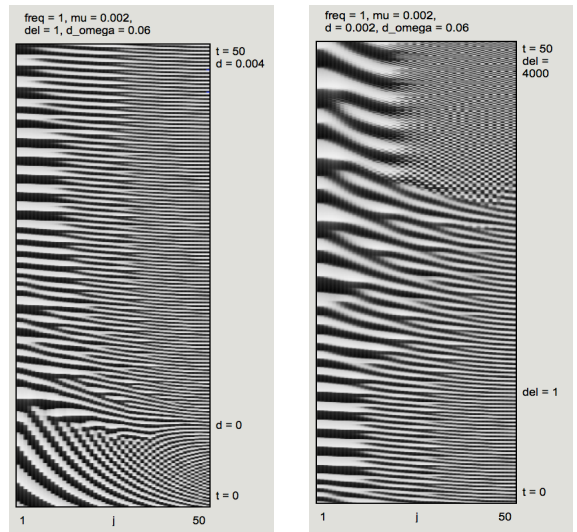


**Figure 11.** Exponentially distributed frequencies

**Figure 12.** Constant coupling, growing delay

Figure 13 shows the evolution of the frequencies with growing coupling strength.

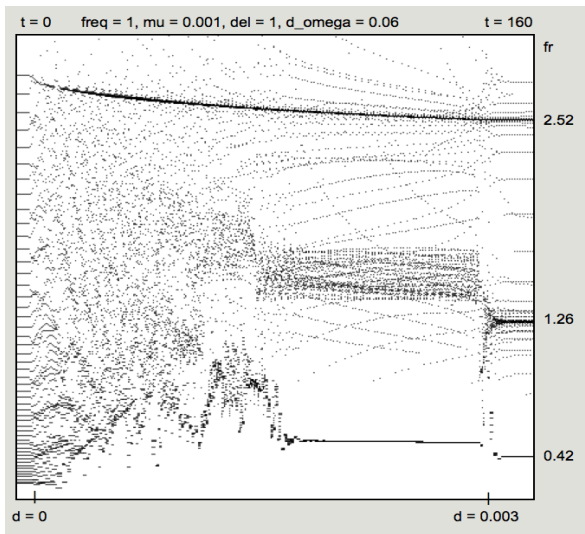


**Figure 13.** Frequencies in a van der Pol chain depending on growing coupling

#### 4. MUSICAL APPLICATIONS

In Neukom's 8-channel studies 21.1-21.9 eight van der Pol oscillators are arranged in a circle and produce the sound for the eight speakers. Each of these oscillators has variable parameters frequency, nonlinearity and a gain and is coupled with his neighbors by variable coupling factors and delay times in both directions. Two additional chains of eight van der Pol oscillators produce control functions which are used for amplitude and frequency modulation. If the frequencies of the oscillators are lower than about 20 Hz the modulations produce pulsations and vibratos. Depending on the coupling strength and the delay some or all pulsations and vibratos synchronize their frequencies. The relative phase which is not audible in audio range plays an important role in the sub-audio range: the pulsations of the single sound sources can have the same frequency but be asynchronous in a rhythmic sense but with growing coupling strength they can produce regular rhythmic patterns, can be exactly in or out of phase.

#### 5. FURTHER INVESTIGATIONS

There are many possibilities for future investigations in this area, e.g. to analytically explain the phenomena described numerically, introduce distinct values for the forward, backward, and self-delays, formulate and investigate a precise model for time- (or state-) dependent delays. Even in the non-delayed case, many open questions remain, such as the precise dependence of the synchronization tree on the various parameters of the model. Moreover, we only considered one-dimensional chains with nearest-neighbor-interactions; other interaction potentials or oscillator topologies could lead to other dynamical phenomena.

#### 6. REFERENCES

- [1] A. Pikovsky, M. Rosenblum, and J. Kurths, *Synchronization*. Cambridge University Press, 2001.
- [2] L. Peltola, C. Erkut, P. R. Cook, and V. Välimäki, "Synthesis of hand clapping sounds," *IEEE Transactions on Audio, Speech, and Language Processing*, vol. 15, no. 3, pp. 1021–1029, 2007.
- [3] C. Huygens, *Horologium Oscillatorium*. Apud F. Muguet, 1673.
- [4] B. van der Pol, "Theory of the amplitude of free and forced triode vibration," *Radio Rev.*, vol. 1.
- [5] E. V. Appleton, "The automatic synchronization of triode oscillators," *Proc. Cambridge Phil. Soc.*, vol. 21, no. 231.
- [6] A. Henrici and M. Neukom, "Synchronization in networks of delayed oscillators," in *Proceedings of the 42th Computer Music Conference ICMC*, 12. - 16. September 2016, Utrecht, Netherlands, 2016.
- [7] S. H. Strogatz, *Sync: The Emerging Science of Spontaneous Order*. Hyperion Press, 2003.
- [8] A. Arenas, A. Diaz-Guilera, J. Kurths, Y. Moreno, and C. Zhou, "Synchronization in complex networks," *Physics Reports*, vol. 469, no. 3, pp. 93–153, 2008.
- [9] J. Pantaleone, "Synchronization of metronomes," *Am. J. Phys.*, vol. 70, no. 10, pp. 992–1000, 2002.
- [10] <https://www.youtube.com/watch?v=5v5eBf2KwF8>, accessed: 2016-04-13.
- [11] M. Neukom, "Applications of synchronization in sound synthesis," in *Proceedings of the 8th Sound and Music Computing Conference SMC*, 6. - 9. July 2011, Padova, Italy, 2011.
- [12] —, *Signals, Systems and Sound Synthesis*. Peter Lang, 2013.
- [13] G. V. Osipov, J. Kurths, and C. Zhou, *Synchronization in Oscillatory Networks*. Springer-Verlag, 2007.
- [14] F. M. Atay, "Van der pol's oscillator under delayed feedback," *J. Sound and Vibration*, vol. 218, no. 2, pp. 333–339, 1998.
- [15] K. Hu and K. Chung, "On the stability analysis of a pair of van der pol oscillators with delayed self-connection, position and velocity couplings," *AIP Advances*, vol. 3, p. 112118, 2013.
- [16] M. Lakshmanan and D. Senthilkumar, *Dynamics of Nonlinear Time-Delay Systems*. Springer-Verlag, 2010.
- [17] F. M. Atay, *Complex Time-Delay Systems: Theory and Applications*. Springer-Verlag, 2010.
- [18] [https://www.zhdk.ch/index.php?id=icst\\_downloads](https://www.zhdk.ch/index.php?id=icst_downloads), accessed: 2016-04-10.